Chapter 7

The Discontinuous Galerkin (DG) Method

The discontinuous Galerkin method has been introduced in previous chapters as a technique for slicing space-time into slabs, on which the solution can be computed sequentially, in time-stepping fashion. Here we will investigate the discontinuous Galerkin method as a spatial discretization method.

The discontinuous Galerkin method is attributed to Reed and Hill [203] who applied it to problems of neutron transport. Unfortunately, this work was never published in the open literature and the method took a long time to attract attention. Early works included Lesaint and Raviart [174] and Johnson, Nävert and Pitkaranta [165], which introduced it into the stabilized methods literature.

7.1 A One-Dimensional Model Problem of Pure Advection

Consider the "reduced problem" of pure advection:

$$u\phi_{,x} = f \qquad \text{on }]0, L[\tag{7.1}$$
$$\phi(0) = g_0 \tag{7.2}$$

where u is a positive constant, and $f = f(x)$ and g_0 are given data. We want to describe the discontinuous Galerkin method for this problem. We note that we previously described the discontinuous Galerkin method for the following ordinary differential equation (ODE) in time (see Section 3.6.2):

$$\dot{y} + \lambda y = F \qquad \text{on }]0, T[\tag{7.3}$$
$$y(0) = y_0 \tag{7.4}$$

These problems are essentially the same in the case when $\lambda = 0$. The equivalence of the two problems is summarized in Table 7.1, and the discretizations are depicted in Figure 7.1. The

Reduced problem	ODE
x	t
$[0, L]$	$[0, T]$
$\phi(x)$	$y(t)$
$u\partial/\partial x$	$1\partial/\partial t$
$f(x)$	$F(t)$
g_0	f_0

Table 7.1: Comparison of the pure advection problem and ODE problem.

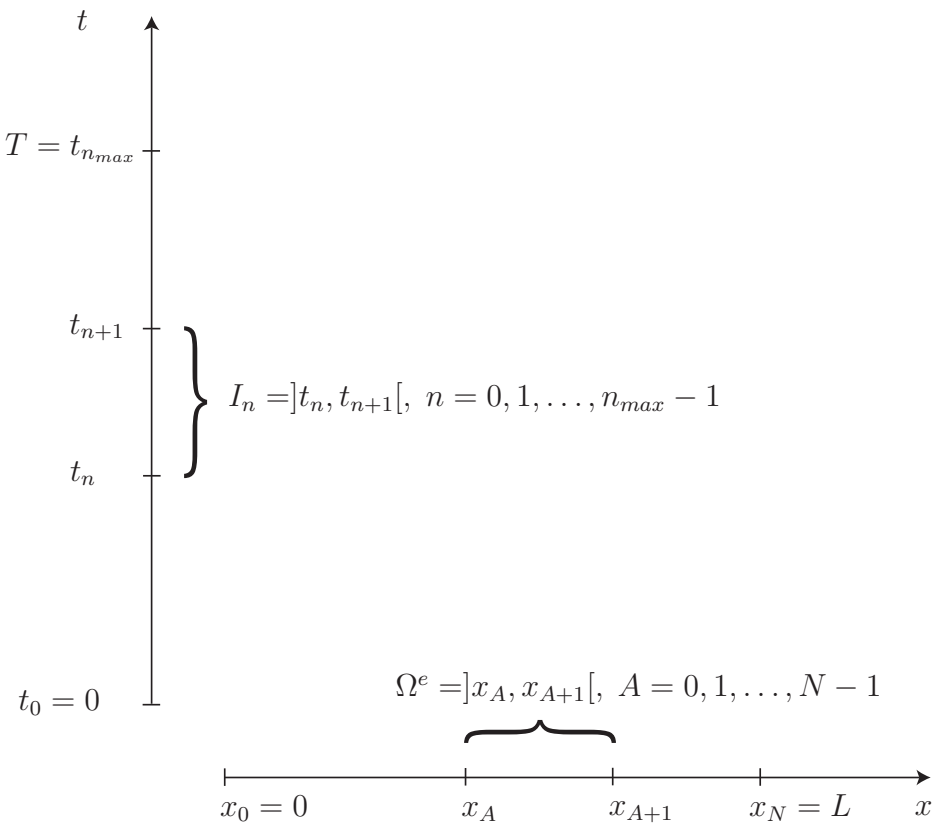

Figure 7.1: Discretization of the ODE in time and the reduced problem in space.

trial space consists of kth-order polynomial on each element ($k \geq 0$). There is no continuity required across element boundaries. We write

$$\mathcal{V}^h = \bigoplus_{A=0}^{N-1} \mathcal{P}^k(]x_A, x_{A+1}[) \tag{7.5}$$

We think of this as an approximation to the "broken space"

$$\mathcal{V} = \bigoplus_{A=0}^{N-1} H^1(]x_A, x_{A+1}[) \tag{7.6}$$

It is a simple matter to describe the discontinuous Galerkin method for the reduced problem. We need simply to mimic the previous developments for the ODE presented in Section 3.6.2. Here is the main equation:

Local formulation

$$B(w^h, \phi^h)_A = L(w^h)_A \qquad A = 0, 1, \ldots, N-1 \tag{7.7}$$

where

$$B(w^h, \phi^h)_A = \int_{x_A}^{x_{A+1}} \left(-u w^h_{,x} \phi^h\right)\, dx + w^h(x^-_{A+1}) u \phi^h(x^-_{A+1}) \tag{7.8}$$

$$L(w^h)_A = \int_{x_A}^{x_{A+1}} w^h f\, dx + w^h(x^+_A) u \phi^h(x^-_A) \tag{7.9}$$

and

$$\phi^h(x^-_0) \stackrel{\text{def}}{=} \phi(0) = g_0 \tag{7.10}$$

We remind the reader that it is crucially important to distinguish between values of functions to the left and right of element boundary nodes, e.g., $w^h(x^-_A)$ and $w^h(x^+_A)$, due to the fact that the functions are discontinuous. Equations (7.7)–(7.9) pertain to element $\Omega^e =]x_A, x_{A+1}[$. Unlike the continuous Galerkin method, the variational equation for individual elements can be isolated in the discontinuous Galerkin method. Of course, to solve this equation requires information from contiguous elements, but in the present case only $\phi^h(x^-_A)$. The Euler-Lagrange form of (7.7)–(7.9), obtained by integration-by-parts, reveals the weighted residual structure of the method, viz.,

$$0 = \int_{x_A}^{x_{A+1}} w^h \underbrace{\left(u\phi^h_{,x} - f\right)}_{\substack{\text{differential} \\ \text{equation} \\ \text{residual}}} dx + w^h(x^+_A) \underbrace{\left(u\phi^h(x^+_A) - u\phi^h(x^-_A)\right)}_{\text{advective flux residual}} \tag{7.11}$$

Equation (7.11) implies weak satisfaction of the differential equation (7.1) on the element interior, and weak continuity of advective flux across the element *inflow boundary*, which in the present case is equivalent to weak enforcement of the continuity of ϕ^h itself. For $A = 0$, the weak enforcement of the continuity of ϕ^h becomes the boundary condition, (7.2).

Remark 7.1 *Note that the weak continuity is enforced on the* ***upwind*** *boundary of the element. This is the key to obtaining a stable formulation. On the other hand, if the continuity condition had been weakly enforced on the downwind boundary of the element, the method would be unconditionally unstable. If the continuity condition had been weakly enforced an both boundaries simultaneously a centered approximation would have been attained and stability would exhibit similar behavior to the continuous Galerkin method. For these reasons, Brezzi* et al. *[31] have pointed out that the discontinuous Galerkin method for first-order equations, with the usual choice of upwind enforcement of continuity, should be viewed as a stabilized method.*

Global formulation

The equations of the *global* method are simply obtained by adding the *local* equations (i.e., (7.7)–(7.9)), and using (7.10). The result is (cf. (3.156) and (3.157)): Find $\phi^h \in \mathcal{V}^h$ such that

$$\mathbf{B}(w^h, \phi^h) = \mathbf{L}(w^h) \qquad \forall w^h \in \mathcal{V}^h \tag{7.12}$$

where

$$\begin{aligned} \mathbf{B}(w^h, \phi^h) &= \sum_{A=0}^{N-1} \left(w^h(x_{A+1}^-) u \phi^h(x_{A+1}^-) - \int_{x_A}^{x_{A+1}} u w_{,x}^h \phi^h \, dx \right) \\ &\quad - \sum_{A=1}^{N-1} w^h(x_A^+) u \phi^h(x_A^-) \end{aligned} \tag{7.13}$$

$$\mathbf{L}(w^h) = w^h(0^+) u g_0 + \sum_{A=0}^{N-1} \int_{x_A}^{x_{A+1}} w^h f \, dx \tag{7.14}$$

The *consistency* of the method is obvious from the Euler-Lagrange form (7.11). Consequently, we may write

$$B(w, \phi)_A = L(w)_A \qquad \forall w^h \in H^1(]x_A, x_{A+1}[), \; A = 0, 1, \ldots, N-1 \tag{7.15}$$

and

$$\mathbf{B}(w, \phi) = \mathbf{L}(w) \qquad \forall w \in \mathcal{V} \tag{7.16}$$

Error orthogonality immediately follows, that is $\mathbf{B}(w^h, e) = 0, \forall w^h \in \mathcal{V}^h$, where $e = \phi^h - \phi$. The *stability* of the method is encompassed in the statement

$$\mathbf{B}(w^h, w^h) = \|w^h\|^2 \qquad \forall w^h \in \mathcal{V}^h \tag{7.17}$$

where

$$\|w^h\|^2 = \frac{u}{2} \left(w^h(L^-)^2 + w^h(0^+)^2 + \sum_{A=1}^{N-1} [\![w^h(x_A)]\!]^2 \right) \tag{7.18}$$

and

$$[\![w^h(x_A)]\!] = w^h(x_A^+) - w^h(x_A^-) \tag{7.19}$$

(Recall, $[\![\cdot]\!]$ is referred to as the "jump operator".)

Remark 7.2 *Note that the stability condition provides control of w^h at the beginning and end of the global interval $]0, L[$ and control of the jump in w^h across element interfaces, but provides* ***no*** *control over w^h in element interiors.*

Remark 7.3 *The solution can be computed on an element-by-element basis, marching from left to right.*

Stabilization

Stabilized discontinuous Galerkin methods are obtained in the usual way:

Local formulation

$$B_{STAB}(w^h, \phi^h)_A = L_{STAB}(w^h)_A \qquad A = 0, 1, \ldots, N-1 \tag{7.20}$$

where

$$B_{STAB}(w^h, \phi^h)_A = B(w^h, \phi^h)_A + \int_{x_A}^{x_{A+1}} u w^h_{,x} \tau u \phi^h_{,x} \, dx \tag{7.21}$$

$$L_{STAB}(w^h)_A = L(w^h)_A + \int_{x_A}^{x_{A+1}} u w^h_{,x} \tau f \, dx \tag{7.22}$$

in which

$$\tau \mid_{]x_A, x_{A+1}[} = \frac{h_A}{2u} \tag{7.23}$$

and

$$h_A = x_{A+1} - x_A \tag{7.24}$$

Global formulation

$$\mathbf{B}_{STAB}(w^h, \phi^h) = \mathbf{L}_{STAB}(w^h) \qquad \forall w^h \in \mathcal{V}^h \tag{7.25}$$

where

$$\mathbf{B}_{STAB}(w^h, \phi^h) = \mathbf{B}(w^h, \phi^h) + \sum_{A=0}^{N-1} \int_{x_A}^{x_{A+1}} u w^h_{,x} \tau u \phi^h_{,x} \, dx \tag{7.26}$$

$$\mathbf{L}_{STAB}(w^h) = \mathbf{L}(w^h) + \sum_{A=0}^{N-1} \int_{x_A}^{x_{A+1}} u w^h_{,x} \tau f \, dx \tag{7.27}$$

The *stability* of the method is given by the relation

$$\mathbf{B}_{STAB}(w^h, w^h) = \| w^h \|^2_{STAB} \qquad \forall w^h \in \mathcal{V}^h \tag{7.28}$$

where

$$\| w^h \|^2_{STAB} = \| w^h \|^2 + \sum_{A=0}^{N-1} \int_{x_A}^{x_{A+1}} \tau \left(u w^h_{,x} \right)^2 \, dx \tag{7.29}$$

It can be seen that stabilization strengthens stability on element interiors. *Consistency* is obvious and error orthogonality immediately follows, namely,

$$\mathbf{B}_{STAB}(w^h, e) = 0 \qquad \forall w^h \in \mathcal{V}^h \tag{7.30}$$

where $e = \phi^h - \phi$.

Exercise 7.1 (Convergence of the stabilized discontinuous Galerkin method.) *Using an interpolation estimate in the form,*

$$|\eta|_{H^l(]x_A, x_{A+1}[)} \leq \tilde{c}\, h_A^{k+1-l} |\phi|_{H^{k+1}(]x_A, x_{A+1}[)} \tag{7.31}$$

where η is the interpolation error and $\tilde{c}$ is a constant, prove the following error estimate:

$$\| e \|_{STAB} \leq c \left(\sum_{A=0}^{N-1} h_A^{2k+1} |\phi|^2_{H^{k+1}(]x_A, x_{A+1}[)} \right)^{1/2} \tag{7.32}$$

where c is a constant. State all hypothesis (Hint: Use the proof for the ODE case in Section 3.6.2 as a model. For an alternate proof see Engel et al. [70].)

Conservation

Discontinuous Galerkin methods possess local conservation laws. The local conservation laws are particularly prized and some of the good behavior of these methods is attributed to them. The basic reason that conservation is an inherent property is that the polynomial basis on each element contains the constant. In other words we can select

$$w^h(x) = 1 \qquad \forall x \in]x_A, x_{A+1}[\tag{7.33}$$

and substitute this into (7.12) or (7.25), resulting in

$$\boxed{u\phi^h(x_{A+1}^-) = u\phi^h(x_A^-) + \int_{x_A}^{x_{A+1}} f \, dx} \tag{7.34}$$

The addition of the stabilizing term has no effect on conservation in this case. (7.34) is a statement of ***local conservation***. It amounts to an exact first integral of the governing differential equation (7.1), namely

$$\boxed{u\phi(x_{A+1}) = u\phi(x_A) + \int_{x_A}^{x_{A+1}} f \, dx} \tag{7.35}$$

Let us start at the left and progress from element to element using both (7.34) and (7.35):

$A = 0$

$$\begin{aligned} u\phi^h(x_1^-) &= u\phi^h(x_0^-) + \int_{x_0}^{x_1} f\ dx \\ &= u\phi^h(0^-) + \int_0^{x_1} f\ dx \\ &= ug_0 + \int_0^{x_1} f\ dx \end{aligned} \tag{7.36}$$

$$\begin{aligned} u\phi(x_1) &= u\phi(x_0) + \int_{x_0}^{x_1} f\ dx \\ &= u\phi(0) + \int_0^{x_1} f\ dx \\ &= ug_0 + \int_0^{x_1} f\ dx \end{aligned} \tag{7.37}$$

Comparing (7.36) and (7.37), we see that

$$\phi^h(x_1^-) = \phi^h(x_1) \tag{7.38}$$

Thus the numerical solution at x_1^- (i.e., at the *outflow*) is exact. We continue:

$A = 1$

$$\begin{aligned} u\phi^h(x_2^-) &= u\phi^h(x_1^-) + \int_{x_1}^{x_2} f\ dx \\ &= u\phi^h(x_1) + \int_{x_1}^{x_2} f\ dx \end{aligned} \tag{7.39}$$

$$u\phi(x_2) = u\phi(x_1) + \int_{x_1}^{x_2} f\ dx \tag{7.40}$$

Comparing (7.39) and (7.40) we have

$$\phi^h(x_2^-) = \phi^h(x_2) \tag{7.41}$$

The numerical solution at x_2^- is also exact. The pattern should now be clear. Proceeding from element to element, we can show that

$$\phi^h(x_A^-) = \phi^h(x_A) \qquad A = 0, 1, \ldots, N \tag{7.42}$$

The result is depicted schematically in Figure 7.2. It holds for all orders of approximation (i.e., $k \geq 0$). The case $k = 0$ dramatizes the difference in approximation quality of inflow and outflow values of the solution (see Fig. 7.3).

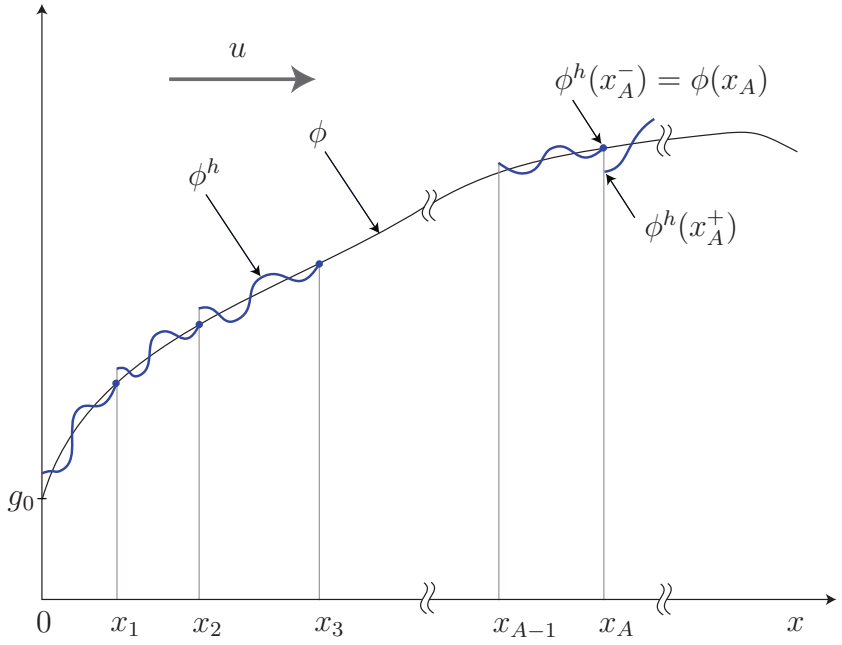

Figure 7.2: The element outflow values are exact for the discontinuous Galerkin method applied to the reduced problem of pure advection, with *or* without stabilization. This property is a consequence of local conservation. Schematically depicted is a high-order discretization, say $k \geq 4$.

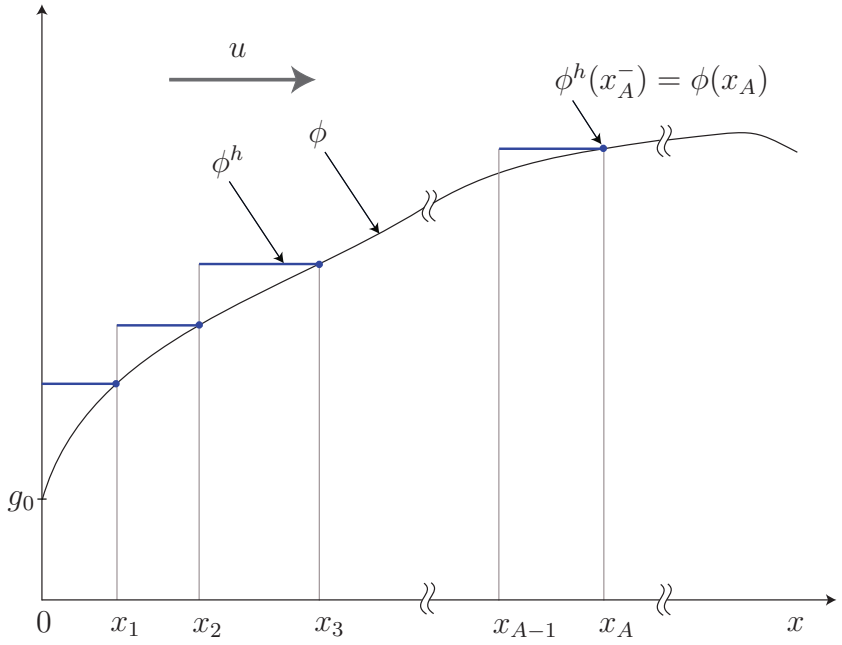

Figure 7.3: Solution of the discontinuous Galerkin method for the case $k = 0$. The element outflow values of the numerical solution are exact.

Global conservation can be derived by setting

$$w^h(x) = 1 \qquad \forall x \in]0, L[\tag{7.43}$$

in either (7.12) or (7.25):

$$\sum_{A=0}^{N-1} u\phi^h(x_{A+1}^-) - \sum_{A=1}^{N-1} u\phi^h(x_A^-) = ug_0 + \int_0^L f \, dx \tag{7.44}$$

Changing the indexing on the first term results in

$$\begin{aligned} ug_0 + \int_0^L f \, dx &= \sum_{A=1}^{N} u\phi^h(x_A^-) - \sum_{A=1}^{N-1} u\phi^h(x_A^-) \\ &= u\phi^h(x_N^-) \\ &= u\phi^h(L^-) \end{aligned} \tag{7.45}$$

$$\boxed{u\phi^h(L^-) = ug_0 + \int_0^L f \, dx} \tag{7.46}$$

This is also an exact integral as may be seen by integrating (7.1):

$$\boxed{u\phi(L) = ug_0 + \int_0^L f \, dx} \tag{7.47}$$

Robustness

The advection problem (7.1)–(7.2) was solved by the discontinuous Galerkin method (DGM) and stabilized discontinuous Galerkin method (SDGM) for different orders of interpolation (i.e., k). The domain $]0, 1[$ was discretized into ten equal-length elements, and a Dirac delta distribution was applied at various points within the third element (i.e., in the interval $]0.3, 0.4[$). The problems solved is stated as follows: Find ϕ such that

$$1\phi_{,x} = \delta(x, y) \, , \qquad \forall x \in]0, 1[\tag{7.48}$$

$$\phi(0) = 1 \tag{7.49}$$

where $0.3 < y < 0.4$. The exact solution is

$$\phi(x) = 1 + H(x - y) \tag{7.50}$$

where H is the *Heaviside function*, namely

$$H(x - y) = \begin{cases} 0 & x < y \\ 1 & x > y \end{cases} \tag{7.51}$$

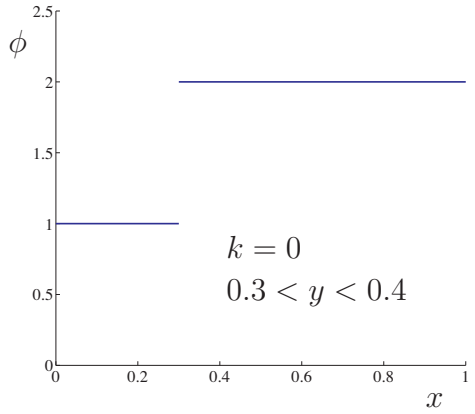

Figure 7.4: Discontinuous Galerkin method for advection with constant interpolation ($k = 0$).

Monotonicity and Continuity

The DGM with constant interpolation is the only method which retains the monotonicity of the exact solution (see Fig. 7.4). For $k \geq 1$, monotonicity is lost (see Figs. 7.5–7.7). Stabilization improves the approximate solution (Fig. 7.5) and yields monotonicity and continuity in the linear case in the limit $\tau \mapsto \infty$. For higher-order interpolation ($k \geq 2$), however, monotonicity is lost both for the DGM and SDGM (see Figs. 7.6–7.7). The SDGM yields continuity in the limit as $\tau \mapsto \infty$, but not monotonicity. In other words, least-squares stabilization cannot ensure an adequate approximation of the solution for higher-order interpolation in the element where the Dirac delta distribution is located. One also concludes that higher-order methods are *not* the methods of choice in the case of shocks, and that constant interpolation most closely reflects the character of the exact solution.

Dependence on Location of Dirac Delta Distribution

For constant interpolation, the approximation is independent of the location of the Dirac delta distribution within the element (Fig. 7.4). For $k \geq 1$, the approximations of the DGM and SDGM strongly depend on the location y of the Dirac delta distribution. When the Dirac delta distribution is very close to an upwind node, the DGM yields more accurate results than the SDGM, which can be seen for the case of cubic interpolation in Figure 7.7(a). In the case when the Dirac delta distribution in close to a downwind node, the results of the SDGM are better than those of the DGM (Fig. 7.7(b)). Again, constant interpolation yields the best results, and the results for linear interpolation with stabilization are acceptable.

Localization Property

An important observation from Figures 7.4–7.7 is that for advection, both DGM and SDGM *localize* the non-monotonicity within one single element. The solution at the outflow boundary of the element containing the Dirac delta distribution is exact for all k. This follows from local conservation.

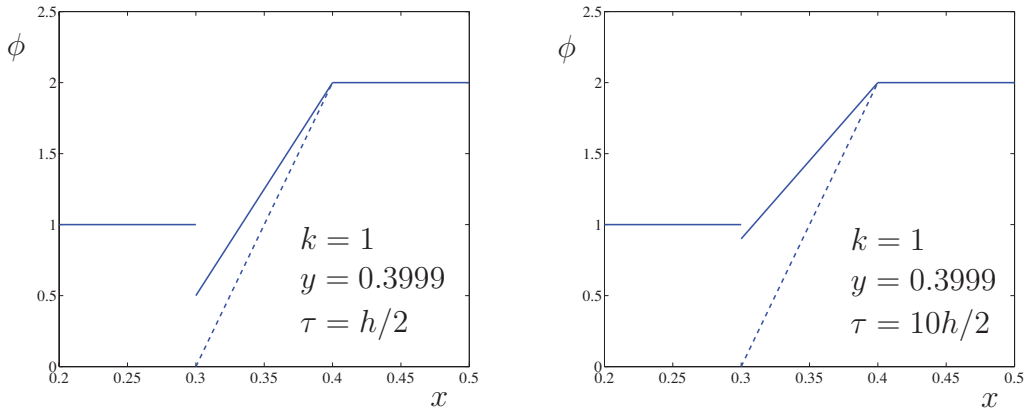

(a) (b)

Figure 7.5: Discontinuous and stabilized discontinuous Galerkin methods for advection with linear interpolation ($k = 1$). The continuous line indicates the SDGM, the dashed line indicates DGM.

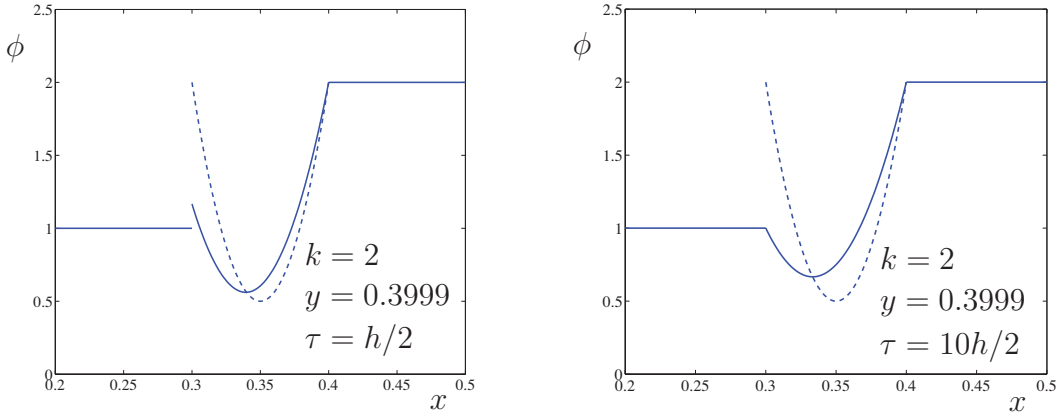

(a) (b)

Figure 7.6: Discontinuous and stabilized discontinuous Galerkin methods for advection with quadratic interpolation ($k = 2$). The continuous line indicates the SDGM, the dashed line indicates DGM.

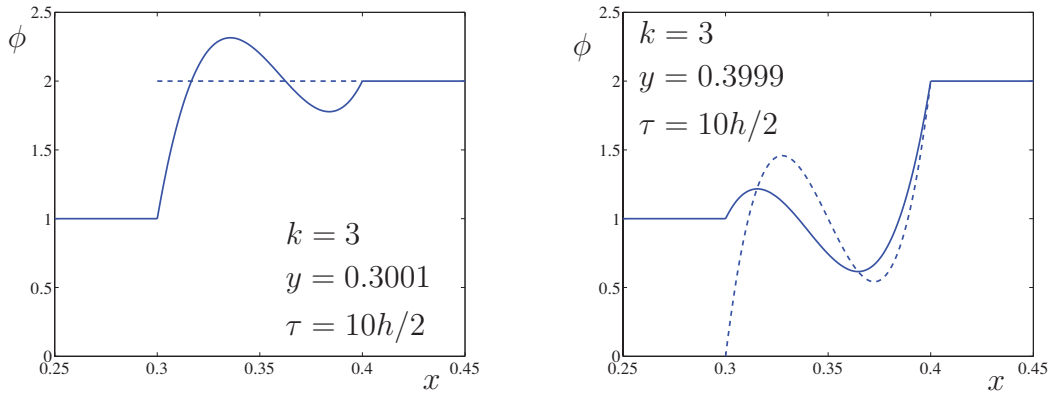

(a) (b)

Figure 7.7: Discontinuous and stabilized discontinuous Galerkin methods for advection with cubic interpolation ($k = 3$). The continuous line indicates the SDGM, the dashed line indicates DGM.

7.2 A One-Dimensional Model Problem of Pure Diffusion

Consider the following diffusion model problem:

$$-\kappa\phi_{,xx} = f \qquad \text{on }]0, L[\tag{7.52}$$
$$\phi(0) = g_0 \tag{7.53}$$
$$\phi(L) = g_L \tag{7.54}$$

where κ is a positive constant, $f = f(x)$, and g_0 and g_L are given boundary data.

The set-up and spaces $\mathcal{V}$ and $\mathcal{V}^h$ are the same as for the pure advection problem described previously. Let the *diffusive flux* at element boundaries be denoted

$$\kappa\phi^h_{,n}(x_A^{\pm}) = \kappa\phi^h_{,x}(x_A^{\pm})n(x_A^{\pm}) \tag{7.55}$$
$$n(x_A^{\pm}) = \mp 1 \tag{7.56}$$

Likewise, we write

$$\kappa w^h_{,n}(x_A^{\pm}) = \kappa w^h_{,x}(x_A^{\pm})n(x_A^{\pm}) \tag{7.57}$$

In addition, we need to introduce the *mean-value operator*

$$\langle \kappa\phi^h_{,n}(x_A)\rangle = \frac{\kappa\phi^h_{,n}(x_A^+) + \kappa\phi^h_{,n}(x_A^-)}{2} \tag{7.58}$$

In distinction with the pure advection problem, there is no natural way to write a local discontinuous formulation for the diffusion problem. Consequently, we shall begin with a ***global formulation*** comprising several methods which have been proposed:

$$B(w^h, \phi^h) = L(w^h) \qquad \forall w^h \in \mathcal{V}^h \tag{7.59}$$

where

$$\begin{aligned} B(w^h,\phi^h) &= \sum_{A=0}^{N-1}\int_{x_A}^{x_{A+1}} w^h_{,x}\kappa\phi^h_{,x}\,dx \\ &\quad -w^h(L^-)\kappa\phi^h_{,n}(L^-) - w^h(0^+)\kappa\phi^h_{,n}(0^+) \\ &\quad +\beta\kappa w^h_{,n}(L^-)\phi^h(L^-) + \beta\kappa w^h_{,n}(0^+)\phi^h(0^+) \\ &\quad +\sum_{A=1}^{N-1}[\![w^h(x_A)]\!]\langle\kappa\phi^h_{,n}(x_A)\rangle + \beta\sum_{A=1}^{N-1}\langle\kappa w^h_{,n}(x_A)\rangle[\![\phi^h(x_A)]\!] \\ &\quad +\tau_N w^h(L^-)\phi^h(L^-) + \tau_0 w^h(0^+)\phi^h(0^+) \\ &\quad +\sum_{A=1}^{N-1}\tau_A[\![w^h(x_A)]\!][\![\phi^h(x_A)]\!] \end{aligned} \tag{7.60}$$

$$\begin{aligned} L(w^h) &= \sum_{A=0}^{N-1}\int_{x_A}^{x_{A+1}} w^h f\,dx \\ &\quad +\beta\kappa w^h_{,n}(L^-)g_L \\ &\quad +\beta\kappa w^h_{,n}(0^+)g_0 \\ &\quad +\tau_N w^h(L^-)g_L \\ &\quad +\tau_0 w^h(0)^+ g_0 \end{aligned} \tag{7.61}$$

in which β is a parameter defining the particular method, τ is the dimensional stabilization parameter, given by

$$\tau_0 = \gamma\frac{\kappa}{h_0} \tag{7.62}$$

$$\tau_N = \gamma\frac{\kappa}{h_N} \tag{7.63}$$

$$\tau_A = 2\gamma\frac{\kappa}{h_{A-1}+h_A}, \qquad A = 1,2,\ldots,N-1 \tag{7.64}$$

and $\gamma \geq 0$ is a (non-dimensional) stabilization parameter.

Remark 7.4 *If $\gamma = 0$ and $\beta = -1$, (7.59)–(7.64) yield a symmetric method known as the Global Element Method (Delves and Hall [61]). Setting $\gamma = 0$ and $\beta = 1$ yields the method of Oden, Babuška and Baumann [194] in which the interface terms constitute a skew-symmetric operator. If $\beta = -1$ and $\gamma > 0$, we obtain the interior penalty collocation method (see Wheeler [259]), a generalization of Nitsche's method to the elliptic problem (see Nitsche [189], Stenberg [231, 232]), generalized to the discontinuous case. See Arnold et al. [7] for a comprehensive analysis and comparison of these and other methods for the diffusion equation.*

Remark 7.5 *It is somewhat surprising that for diffusion problems the discontinuous Galerkin method is extremely complicated. Contrast this with the continuous Galerkin method in which all terms save the first in (7.60) and (7.61) are zero. It appears that the discontinuous Galerkin method is better suited for first-order differential operators (e.g., those describing advection) rather than second-order differential operators (e.g., those describing diffusion). However, it is important to understand the behavior of the discontinuous Galerkin method on second-order operators because they are included in typical flow equations, such as the advection-diffusion and Navier-Stokes equations.*

Remark 7.6 *Another possibility is to reformulate the second-order problem in a "mixed" format involving first-order equations, and then apply the discontinuous Galerkin method to it. Such a system has the form*

$$\sigma_{,x} + f = 0 \tag{7.65}$$

$$\sigma = \kappa\phi_{,x} \tag{7.66}$$

Both σ and ϕ need to be discretized. See Brezzi and Fortin [33] for background on mixed methods and Hughes, Masud and Wan [135] and Brezzi et al. *[36] for a discontinuous Galerkin method for (7.65)–(7.66).*

Consistency

For sufficiently smooth ϕ it can be shown that

$$B(w^h, e) = 0 \qquad \forall w^h \in \mathcal{V}^h \tag{7.67}$$

where $e = \phi^h - \phi$.

Stability

The relevant norm for the diffusion problem is

$$\begin{aligned} \|w^h\|^2_{STAB} &= \sum_{A=1}^{N-1} \int_{x_A}^{x_{A+1}} \kappa \left(w^h_{,x}\right)^2 \, dx \\ &\quad + \tau_0 \left(w^h(0^+)\right)^2 + \tau_N \left(w^h(L^-)\right)^2 \\ &\quad + \sum_{A=1}^{N-1} \tau_A [\![w^h(x_A)]\!]^2 \end{aligned} \tag{7.68}$$

Convergence

The following error estimate holds for the diffusion problem (see Engel *et al*. [70] for a detailed proof):

$$\|e\|_{STAB} \leq c \left(\sum_{A=0}^{N-1} h_A^{2k} |\phi|^2_{H^{k+1}(]x_A, x_{A+1}[)} \right)^{1/2} \tag{7.69}$$

Robustness

The diffusion problem was solved by the discontinuous Galerkin method (DGM) and by the stabilized discontinuous Galerkin method (SDGM). The domain $]0,1[$ was discretized into ten equal-length elements and a Dirac delta distribution was applied at $y = 0.69$. The statement of the problem is: Find ϕ such that

$$1\,\phi_{,xx} + \delta(x-y) = 0 \qquad \text{on }]0,1[\tag{7.70}$$

$$\phi(0) = 0 \tag{7.71}$$

$$\phi(1) = 0 \tag{7.72}$$

Skew-Symmetric and Symmetric Formulations

We refer to the cases $\beta = -1$ and $\beta = 1$ as the symmetric and skew symmetric cases, respectively. For $\beta = -1$, the entire formulation is symmetric, whereas for $\beta = 1$ only the Galerkin interface terms are skew symmetric, the remaining terms being symmetric. The non-stabilized skew-symmetric method, introduced by Oden, Babuška and Baumann [194], is stable for quadratic and higher-order interpolation. However, as can be seen in Figure 7.8(a) for quadratic interpolation, the approximation can be quite inaccurate in some cases. Increasing the stabilization parameter τ leads to better approximations (see Figs. 7.8(b), 7.8(c)). In the case of linear interpolation, the skew-symmetric method without stabilization is unstable, while good convergence is achieved for the stabilized version.

The stabilization terms (i.e., τ terms) were originally introduced by Nitsche [189]. However, Nitsche's method amounts to the symmetric, rather than the skew symmetric, formulation, which is unstable for τ not sufficiently large. Invoking Nitsche's stabilization terms in the skew-symmetric formulation results in a robust method which seems to yield the best discontinuous approximation to the diffusion problem, as can be seen in Figure 7.8.

Global Pollution

For the diffusion problem, the advantageous localization property of the discontinuous Galerkin method encountered in the advection case is *lost*, and an off-centered Dirac delta distribution in one single element causes a deteriorated approximation globally. This problem can be fixed by increasing τ (Fig. 7.8).

Choice of Stabilization Parameter

In order to obtain a stable discrete formulation for the symmetric formulation ($\beta = -1$), we need to choose τ sufficiently large.

In contrast, the skew-symmetric formulation ($\beta = 1$), is stable for all $\tau > 0$. This is a desirable property, since choosing a suitable τ for the symmetric formulation may be difficult without knowledge of the smallest eigenvalue. Note that the condition number increases for large values of τ, and therefore it is also important not to choose the stabilization parameter too large.

We investigated the minimum and maximum eigenvalues λ of the discrete problem as a function of τ for $\beta = -1$ and $\beta = 1$, and linear, quadratic, and cubic interpolation. In Figure

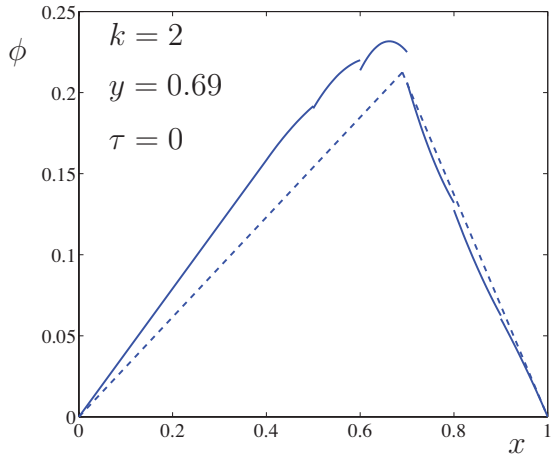

(a) Skew-Symmetric

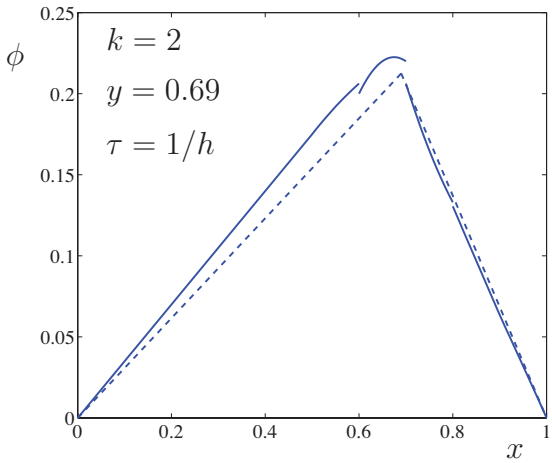

(b) Stabilized Skew-Symmetric

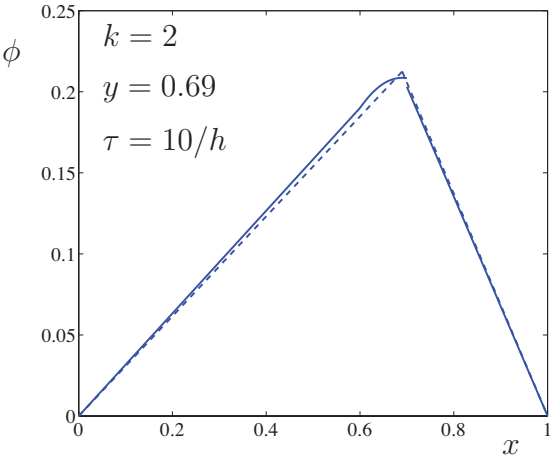

(c) Stabilized Skew-Symmetric

Figure 7.8: Quadratic ($k = 2$) discontinuous Galerkin methods for the diffusion problem. The continuous line represents the exact solution for $\beta = 1$, the dashed line represents the exact solution.

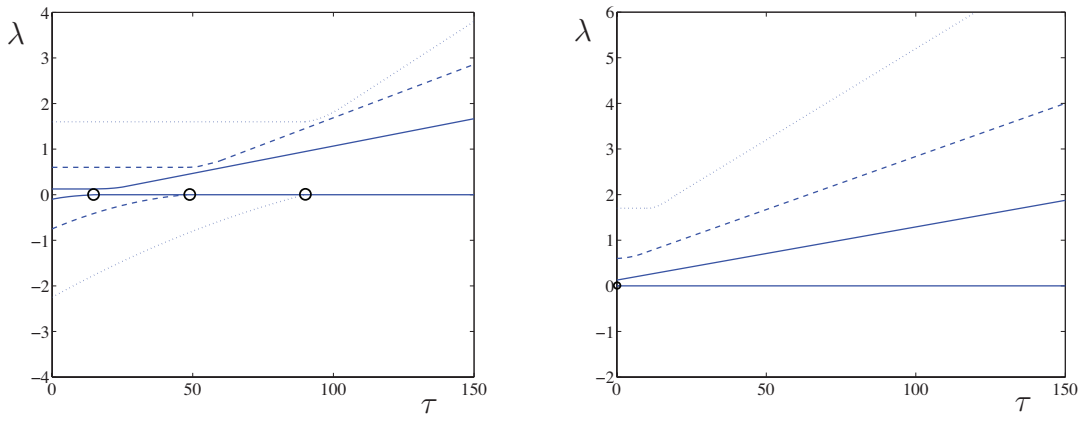

(a) Stabilized Symmetric ($\beta = -1$) (b) Stabilized Skew-Symmetric ($\beta = 1$)

Figure 7.9: Largest and smallest eigenvalue λ as functions of τ (real part of eigenvalues only). The continuous lines indicate $k = 1$, the dashed lines indicate $k = 2$, the dotted lines indicate $k = 3$. The circles in the graphs indicate the value of τ when the smallest eigenvalue becomes positive.

7.9, one can see in each graph the largest and smallest eigenvalues as functions of τ. The circles in the graphs indicate the value of τ when the smallest eigenvalue becomes positive. Note, in particular, that the symmetric formulation is indefinite for τ too small, and that the critical value of τ increases with the order of interpolation. (On the scale of the graphs, the smallest eigenvalue often plots as zero, even though it is positive.)

Efficiency

The number of unknowns of a discretized problem is a good indicator for the efficiency of a numerical method. The discontinuous Galerkin method enables constant interpolation on an element, which is impossible with the continuous Galerkin method, and this is an interesting

k	Quadrilateral	Triangle	Hexahedron	Tetrahedron
0^*	1	2	1	5
1	4	6	8	20
2	2.25	3	3.38	7.14
3	1.78	2.22	2.37	4.35
∞	1	1	1	1

Table 7.2: Number of unknowns for the discontinuous Galerkin method as a multiple of the number of unknowns of the continuous Galerkin method for different elements and orders of interpolation k. For $k = 0$, normalization is with respect to the number of unknowns of the continuous Galerkin method for linear interpolation (i.e., $k = 1$).

possibility for certain problems. Table 7.2 gives an overview of the ratio of the number of unknowns in the discontinuous Galerkin method to the number of unknowns in the continuous Galerkin method for different orders of interpolation k and commonly used two- and three-dimensional elements. In the case of triangles and tetrahedra, the ratio is based on regular meshes obtained from subdivisions of quadrilateral and hexahedral meshes, respectively. For lower-order interpolations, say $k \leq 3$, the discontinuous Galerkin method involves significantly more unknowns than the continuous Galerkin method, but this may be offset by other factors in some cases. Note that, in the limit $k \mapsto \infty$, this ratio approaches 1. *Very* high-order discontinuous Galerkin methods involve a similar number of unknowns as corresponding continuous Galerkin methods.

Remark 7.7 *The proliferation of unknowns of the discontinuous Galerkin method has been viewed as its primary shortcoming. This has motivated the development of the so-called* ***multiscale discontinuous Galerkin method*** *(see Hughes* et al.*'[141], Bochev, Hughes and Scovazzi [22] and Buffa* et al. *[40]), in which the coarse-scale subspaces is taken as continuous, and the fine-scale subspace is discontinuous, and eliminated from the coarse-scale problem by way of local, individual element problems. The end result is a method in which the coarse-scale problem has the same number of unknowns as the continuous Galerkin method but contains stabilization terms due to the discontinuous fine-scale subspace. The performance in most respects is very similar to the discontinuous Galerkin method, but involves many fewer unknowns. A closely related method has been proposed in by Labeur and Wells [169].*

Remark 7.8 *As mentioned previously, the local conservation property of discontinuous Galerkin methods is one of the reasons for their popularity. The implication is that the continuous Galerkin method is not locally conservative. It is often said that the continuous Galerkin method is globally conservative. In the opinion of the authors, these statements are misleading. The local and global conservation structure of the continuous Galerkin method has been studied by Hughes* et al. *[122], Hughes and Wells [147], Cockburn, Karniadakis and Shu [51], and Cockburn and Wandi [52]. It is a subtle topic and the interested reader is referred to these works for further information.*

Remark 7.9 *A comprehensive mathematical study of discontinuous Galerkin methods for the diffusion problem is presented in Arnold* et al. *[7]. Some newer methods are presented in Hughes, Masud and Wan [135], and Brezzi* et al. *[36].*

Remark 7.10 *The discontinuous Galerkin method is a very active area of research. For further information, see Venkatakrishnan* et al. *[255], the review articles by Cockburn [50, 51], and references therein.*

7.3 Multi-dimensional Pure Advection Problem

Let $\Omega = \bigcup_{e=1}^{n_{\rm el}} \Omega^e$, where Ω^e is an element domain, $e = 1, 2, \ldots, n_{\rm el}$, and let $\Gamma = \partial\Omega$ denote its boundary. Likewise, the boundary of element Ω^e is denoted $\Gamma^e = \partial\Omega^e$. The inflow and outflow boundaries are defined as follows:

$$\Gamma_{in} = \{\mathbf{x} \mid \mathbf{x} \in \Gamma \ , \ u_n(\mathbf{x}) = \mathbf{u}(\mathbf{x}) \cdot \mathbf{n}(\mathbf{x}) < 0\} \tag{7.73}$$

$$\Gamma_{out} = \{\mathbf{x} \mid \mathbf{x} \in \Gamma \ , \ u_n(\mathbf{x}) = \mathbf{u}(\mathbf{x}) \cdot \mathbf{n}(\mathbf{x}) \geq 0\} \tag{7.74}$$

where $\mathbf{n}$ is the unit outward normal vector to Γ. The element inflow and outflow boundaries, Γ^e_{in} and Γ^e_{out}, respectively, are defined similarly. The given data are the source $f : \Omega \to \mathbb{R}$, $g : \Gamma_{in} \to \mathbb{R}$, and $\mathbf{u} : \Omega \to \mathbb{R}^{n_d}$, where $n_d \geq 2$ is the number of space dimensions. We assume $\mathbf{u} \in (C^1(\Omega))^{n_d}$ is solenoidal, that is $\nabla \cdot \mathbf{u} = 0$.

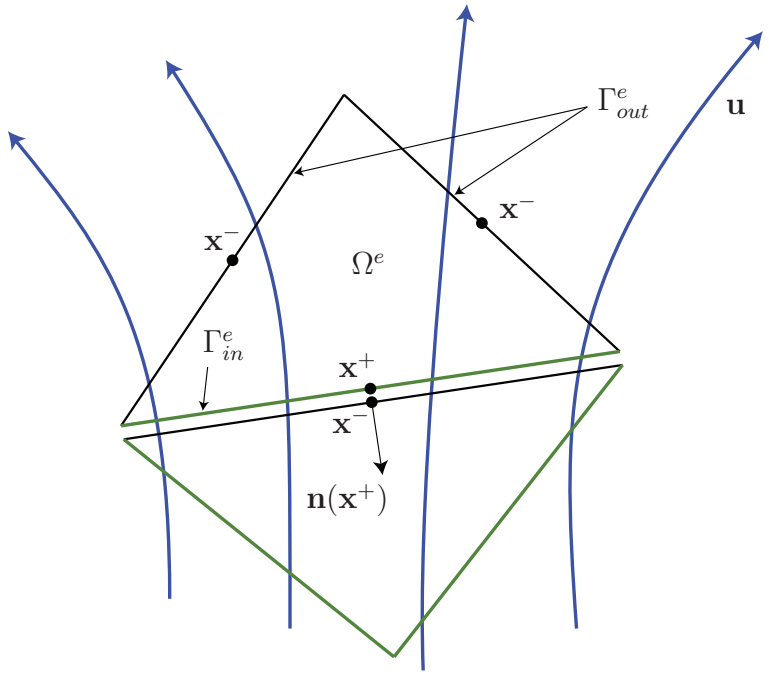

Figure 7.10: We use the notation $\mathbf{x}^+$ and $\mathbf{x}^-$ to denote locations on the inflow and outflow boundaries of a typical element, Ω^e. A contiguous element to Ω^e is shown sharing its inflow boundary. The point $\mathbf{x}^-$ on this element's outflow boundary is located exactly in the same place as the point $\mathbf{x}^+$ shown on Ω^e's inflow boundary, but is separated in the figure for clarity. In general, $w^h(\mathbf{x}^-) \neq w^h(\mathbf{x}^+)$ and $\phi^h(\mathbf{x}^-) \neq \phi^h(\mathbf{x}^+)$ along the interface. When we write $u_n(\mathbf{x}^+)$, we mean $\mathbf{u}(\mathbf{x}) \cdot \mathbf{n}(\mathbf{x}^+)$, that is, along the shared interface $\mathbf{n}(\mathbf{x}^+)$ points away from Ω^e. With this convention, $u_n(\mathbf{x}^-) = \mathbf{u}(\mathbf{x}) \cdot \mathbf{n}(\mathbf{x}^-) = -u_n(\mathbf{x}^+)$.

The multi-dimensional version of the pure advection problem, corresponding to (7.7)–(7.10) is given by

Local formulation

$$B(w^h, \phi^h)_{\Omega^e} = L(w^h)_{\Omega^e} \qquad e = 1, 2, \ldots, n_{\text{el}} \tag{7.75}$$

where

$$B(w^h, \phi^h)_{\Omega^e} = \int_{\Omega^e} \left(-\mathbf{u} \cdot \nabla w^h \, \phi^h\right) \, d\Omega + \int_{\Gamma^e_{out}} u_n(\mathbf{x}^-) w^h(\mathbf{x}^-) \phi^h(\mathbf{x}^-) \, d\Gamma \tag{7.76}$$

$$L(w^h)_{\Omega^e} = \int_{\Omega^e} w^h f \, d\Omega + \int_{\Gamma^e_{in}} u_n(\mathbf{x}^+) w^h(\mathbf{x}^+) \phi^h(\mathbf{x}^+) \, d\Gamma \tag{7.77}$$

and

$$\phi^h(\mathbf{x}^-) = g(\mathbf{x}), \qquad \forall \mathbf{x} \in \Gamma_{in} \tag{7.78}$$

The plus and minus superscripts on $\mathbf{x}$ indicate on which side of the element boundary the function in question is to be evaluated (analogous to the one-dimensional case). Figure 7.10 describes the situation. The remaining results are given in the form of an exercise.

Exercise 7.2 *Following the analogous steps in the one-dimensional case, show that*

(i) ***Euler-Lagrange form***

$$\begin{aligned} 0 = & \int_{\Omega^e} w^h \left(\mathbf{u} \cdot \nabla \phi^h - f\right) d\Omega \\ & + \int_{\Gamma^e_{in}} w^h(\mathbf{x}^+) \left(u_n(\mathbf{x}^+) \phi^h(\mathbf{x}^+) - u_n(\mathbf{x}^+) \phi^h(\mathbf{x}^-)\right) d\Gamma \end{aligned} \tag{7.79}$$

(ii) ***Global formulation***

$$\mathbf{B}(w^h, \phi^h) = \mathbf{L}(w^h) \qquad \forall w^h \in \mathcal{V}^h \tag{7.80}$$

$$\begin{aligned} \mathbf{B}(w^h, \phi^h) = & \sum_{e=1}^{n_{\text{el}}} \left(\int_{\Omega^e} \left(-\mathbf{u} \cdot \nabla w^h \, \phi^h\right) \, d\Omega \right. \\ & + \int_{\Gamma^e_{out}} u_n(\mathbf{x}^-) w^h(\mathbf{x}^-) \phi^h(\mathbf{x}^-) \, d\Gamma \\ & \left. - \int_{\Gamma^e_{in} \setminus \Gamma_{in}} u_n(\mathbf{x}^+) w^h(\mathbf{x}^+) \phi^h(\mathbf{x}^-) \, d\Gamma \right) \end{aligned} \tag{7.81}$$

$$\mathbf{L}(w^h) = \sum_{e=1}^{n_{\text{el}}} \left(\int_{\Gamma^e_{in} \cap \Gamma_{in}} u_n(\mathbf{x}^+) w^h(\mathbf{x}^+) \, g(\mathbf{x}) \, d\Gamma + \int_{\Omega^e} w^h f \, d\Omega \right) \tag{7.82}$$

Consistency/error orthogonality

$$\mathbf{B}(w^h, e) = 0 \qquad \forall w^h \in \mathcal{V}^h \tag{7.83}$$

(iii) ***Stability***

$$\mathbf{B}(w^h, w^h) = |\!|\!| w^h |\!|\!|^2 \qquad \forall w^h \in \mathcal{V}^h \tag{7.84}$$

$$\begin{aligned} |\!|\!| w^h |\!|\!|^2 &= \int_{\Gamma_{in}} |u_n(\mathbf{x}^+)| (w^h(\mathbf{x}^+))^2 \, d\Gamma \\ &\quad + \int_{\Gamma_{out}} |u_n(\mathbf{x}^-)| (w^h(\mathbf{x}^-))^2 \, d\Gamma \\ &\quad + \int_{\Gamma'} |u_n(\mathbf{x})| [\![w^h]\!]^2 \, d\Gamma \end{aligned} \tag{7.85}$$

where

$$\Gamma' = \left(\bigcup_{e=1}^{n_{\text{el}}} \Gamma^e \right) \setminus \Gamma \tag{7.86}$$

$$[\![w^h]\!] = w^h(\mathbf{x}^+) - w^h(\mathbf{x}^-) \tag{7.87}$$

(Note that on Γ_{in}, $u_n(\mathbf{x}^+) = |u_n(\mathbf{x}^+)| > 0$, and on Γ_{out}, $u_n(\mathbf{x}^-) = |u_n(\mathbf{x}^-)| > 0$.)

(iv) ***Stabilized global formulation***

$$\mathbf{B}_{STAB}(w^h, \phi^h) = \mathbf{L}_{STAB}(w^h) \qquad \forall w^h \in \mathcal{V}^h \tag{7.88}$$

$$\mathbf{B}_{STAB}(w^h, \phi^h) = \mathbf{B}(w^h, \phi^h) + \sum_{e=1}^{n_{\text{el}}} \int_{\Omega^e} \mathbf{u} \cdot \nabla w^h \, \tau \, \mathbf{u} \cdot \nabla \phi^h \, d\Omega \tag{7.89}$$

$$\mathbf{L}_{STAB}(w^h) = \mathbf{L}(w^h) + \sum_{e=1}^{n_{\text{el}}} \int_{\Omega^e} \mathbf{u} \cdot \nabla w^h \, \tau \, f \, d\Omega \tag{7.90}$$

τ may be defined element-wise by

$$\tau(\mathbf{x}) = \tau^e(\mathbf{x}) = \frac{h^e}{2\,|\mathbf{u}(\mathbf{x})|} \qquad \forall \mathbf{x} \in \Omega^e \tag{7.91}$$

Consistency/error orthogonality

$$\mathbf{B}_{STAB}(w^h, e) = 0 \qquad \forall w^h \in \mathcal{V}^h \tag{7.92}$$

Stability

$$\mathbf{B}_{STAB}(w^h, w^h) = |\!|\!| w^h |\!|\!|^2_{STAB} \qquad \forall w^h \in \mathcal{V}^h \tag{7.93}$$

$$|\!|\!| w^h |\!|\!|^2_{STAB} = |\!|\!| w^h |\!|\!|^2 + \sum_{e=1}^{n_{\text{el}}} \int_{\Omega^e} \tau \left(\mathbf{u} \cdot \nabla w^h \right)^2 \, d\Omega \tag{7.94}$$

(v) ***Local conservation***

$$\int_{\Gamma^e_{out}} u_n(\mathbf{x}^-) \, \phi^h(\mathbf{x}^-) \, d\Gamma = \int_{\Gamma^e_{in}} u_n(\mathbf{x}^+) \, \phi^h(\mathbf{x}^-) \, d\Gamma + \int_{\Omega^e} f \, d\Omega \tag{7.95}$$

Global conservation

$$\int_{\Gamma_{out}} u_n(\mathbf{x}^-)\,\phi^h(\mathbf{x}^-)\,d\Gamma = \int_{\Gamma_{in}} u_n(\mathbf{x}^+)\,g(\mathbf{x})\,d\Gamma + \int_{\Omega} f\,d\Omega \tag{7.96}$$

(Hint: To obtain (7.96), sum (7.95) over the elements.)

Exercise 7.3 *Consider the multi-dimensional problem of pure advection corresponding to (7.1)–(7.2):*

$$\mathbf{u}\cdot\nabla\phi = f \qquad \forall \mathbf{x}\in\Omega \tag{7.97}$$

$$\phi(\mathbf{x}) = g(\mathbf{x}) \quad \forall \mathbf{x}\in\Gamma_{in} \tag{7.98}$$

where $\mathbf{u}:\Omega\to\mathbb{R}^{n_d}$ *is a smooth, solenoidal vector field such that* $\mathbf{u}(\mathbf{x})\neq 0$, $\forall\mathbf{x}\in\Omega\cup\Gamma_{in}$. *Assume the set of integral curves of* $\mathbf{u}$ *emanating from* Γ_{in} *cover* Ω. *The integral curves of* $\mathbf{u}$ *are defined by*

$$\frac{d\mathbf{x}}{ds}(s) = \mathbf{u}(\mathbf{x}(s)) \tag{7.99}$$

$$\mathbf{x}(0)\in\Gamma_{in} \tag{7.100}$$

Another way to say this is that for each $\mathbf{x}\in\Omega$, *there is a unique integral curve of* $\mathbf{u}$ *through* $\mathbf{x}$ *originating at some point in* Γ_{in}. *Show that:*

$$\phi(\mathbf{x}(s)) = \phi(\mathbf{x}(0)) + \int_0^s f(\mathbf{x}(t))\,dt \tag{7.101}$$

and interpret this result by way of a sketch.